Article

Comparative Study of Greener Alkene Epoxidation Using a Polymer-Supported Mo(VI) Complex: Performance Evaluation and Optimisation via Response Surface Methodology

Md Masud Rana Bhuiyan and Basudeb Saha *

School of Engineering, Lancaster University, Lancaster LA1 4YW, UK; m.m.bhuiyan@lancaster.ac.uk
* Correspondence: b.saha@lancaster.ac.uk

Abstract: A heterogeneous polybenzimidazole-supported Mo(VI) catalyst and *tert*-butyl hydroperoxide (TBHP) as an oxidising reagent have been utilised to establish a more environmentally friendly and greener alkene epoxidation process. A polybenzimidazole-supported Mo(VI) complex (PBI.Mo) has been prepared, characterised and evaluated successfully. The stability and catalytic activity of the produced catalyst have been evaluated for the epoxidation of 1,7-octadiene and 1,5-hexadiene in a jacketed stirred batch reactor to assess its performance towards these alkenes. The suitability and efficiency of the catalyst have been compared by studying the effect of reaction temperature, feed mole ratio of alkene to TBHP, catalyst loading, and reaction time on the yield of 1,2-epoxy-5-hexene and 1,2-epoxy-7-octene. Response surface methodology (RSM) using Box–Behnken Design (BBD) has been employed to design experimental runs and study the catalytic performance of the PBI.Mo catalyst for all batch experimental results. A quadratic regression model has been developed representing an empirical relationship between reaction variables and response, which is the yield of epoxides. The numerical optimisation technique concluded that the maximum yield that can be reached is 66.22% for 1,7-octadiene and 64.2% for 1,5-hexadiene. The reactivity of alkenes was observed to follow the sequence 1,5-hexadiene > 1,7-octadiene. The findings of this study confirm that the optimal reaction conditions vary between the two reactions, indicating differences in catalytic performance for each alkene.

Keywords: alkene epoxidation; polymer-supported Mo(VI) catalyst; 1,7-octadiene; 1,5-hexadiene; response surface methodology (RSM)

1. Introduction

Over the past few decades, research on organic polymers has been conducted to investigate the immobilisation of catalytically active metal species [1–4]. For a polymer-supported catalyst to be used in continuously operating processes, it must have great long-term stability in addition to high activities and selectivity. Silica, graphene oxide, zeolites, layered doubled hydroxide (LDH), hydroxyapatite (HAP), alumina, ion-exchange resins, polymers, and metal–organic frameworks are examples of organic or inorganic materials on which catalytically active metal species have been immobilised to develop suitable heterogeneous catalysts for epoxidation [5–17]. In recent times, polymer-supported heterogeneous catalysts have demonstrated significant catalytic activity and product selectivity when employed in the manufacture of epoxides, with alkyl hydroperoxide acting

as an oxidant [15,18]. Due to polymers' stability, inertness, nontoxicity, and insoluble nature, polymers have attracted attention as potential substrates for catalysts [19]. Nevertheless, there does not seem to be any research on the epoxidation of 1,5-hexadiene and 1,7-octadiene with *tert*-butyl hydroperoxide as an oxidising reagent in the presence of polymer-supported Mo(VI) catalyst despite several published studies on polymer-supported Mo(VI) catalysts in the epoxidation of various other alkene substrates.

Since alkene epoxidation allows for the direct oxidation of two adjacent carbon atoms from an alkene using catalysts made of transition metal complexes and oxidising agents like hydroperoxides, peracids, or molecular oxygen in the presence of oxidising reagents, it has been established as the most important stage in chemical synthesis [20–22]. By opening the epoxide ring, the three-membered ring unit of epoxide demonstrates simple elaboration to valuable additional functionality [23]. Epoxides play an important role in the context of biological activity and are very valuable as precursors for the development of drugs, agrochemicals, and additives [24]. Alkene epoxidation is a very useful reaction in industrial organic synthesis as it is the precursor in the synthesis of various important substances like plasticizers, perfumes, and epoxy resins [25]. The synthesised 1,2-epoxy-5-hexene also can be used as a raw material or an intermediate. One of the key aspects of 1,2-epoxy-5-hexene is that it serves as a dual-functional monomer that helps in cross-linking the polysiloxane network, and 1,2-epoxy-5-hexene-incorporated polysiloxane can be actively employed as a high-brightness light emitting diodes (LED) encapsulant [26]. 1,2-epoxy-5-hexene was photopolymerised to create novel hydrogels, which were then evaluated for their viscoelastic characteristics in preparation for possible tissue replacement applications [27]. Another important use of 1,2-epoxy-5-hexene is that it can be used in enzymatic esterification of an acid. This product can easily be substituted in the α-carbon by an amino group to obtain 2- aminoesters, the latter being useful as an intermediate reagent in the synthesis of many drugs such as Taxol, a powerful anticancer drug [28]. Another epoxide, which is 1,2-epoxy-7-octene, serves as a useful monomer, as its internal double bond permits further modifications or polymerisation [29]. Both 1,2-epoxy-5-hexene and 1,2-epoxy-7-octene are utilised to synthesise epoxy-based silicone prepolymers, which serve as the basis for UV-curable coatings with tunable properties [30]. Research indicates potential applications of these epoxide-derived polymers in drug delivery [31].

The traditional epoxidation process in fine chemical industries uses stoichiometric peracids, such as peracetic acid and m-chloroperbenzoic acid or chlorohydrin, as oxidising agents in batch reactions in liquid phases [32,33]. Because chlorohydrin generates chlorinated by-products and peracids produce a similar quantity of acid waste, this procedure has the disadvantage of not being environmentally friendly when utilising these reagents [33]. Additionally, there are security concerns related to the handling and storage of peracid [15]. The Halcon process, which is catalysed by homogeneous Mo(VI) or heterogeneous Ti(IV) supported on SiO2, is another important liquid-phase epoxidation [34]. Due to corrosion and deposition on the reactor, as well as significant requirements in terms of work-up, product isolation, and purification techniques, homogeneous catalysed epoxidation methods are not economically viable for industrial applications [35]. There is a great need for safer epoxidation processes that generate little waste. Because of this, efforts have been made to develop more environmentally friendly and effective epoxidation processes that use a heterogeneous catalyst and a safe oxidant.

In this process, an efficient and selective polybenzimidazole-supported molybdenum (VI) complex (PBI.Mo) was used as a catalyst for the batch epoxidation of 1,5-hexadiene and 1,7-octadiene. This system is free of solvents and uses the environmentally friendly TBHP as an oxidant [36]. Using TBHP as an oxidant, the catalysts were also investigated in batch investigations using a range of alkenes and reaction conditions.

Experiments were carried out to study the effect of different parameters, including reaction temperature, feed molar ratio of alkene to TBHP, and catalyst loading on the yield of 1,2-epoxy-5 hexene and 1,2-epoxy-7-octene, to optimise the reaction conditions in a classical batch reactor. A quadratic regression model was developed representing an empirical relationship between reaction variables and response. Response surface methodology (RSM) using Box–Behnken Design (BBD) was employed to design experimental runs and study the interaction effect of different variables on the reaction response.

2. Materials and Methods

2.1. Materials

Sodium hydroxide (purum p.a. ≥98%), deionised water, acetone, molybdenyl acetylacetonate ($MoO_2(acac)_2$) (99%), toluene (anhydrous, 99.8%), 1,5-hexadiene (97%), 1,7-octadiene (97%), and *tert*-butyl hydroperoxide (TBHP) solution in water (70% (*w/w*)) were purchased from SigmaAldrich (Merck Life Science UK Limited, Gillingham). and gas chromatography (GC) was used to verify the purity of the chemicals. Microporous polybenzimidazole (PBI) resin beads were supplied by Celanese Corporation, Texas, USA. The water content of TBHP was removed by a Dean–Stark apparatus from the toluene solution, and the concentration of the resulting TBHP solution was determined by iodometric titration [37]. The concentration of TBHP in toluene was found to be 3.57 mol L^{-1}. The quantification of samples collected from the reactor was carried out using the internal standard method in the GC, and *iso*-octane (anhydrous, 99.8%) was used as an internal standard.

2.2. Synthesis of Polymer-Supported Mo(Vi) Catalyst

Being able to withstand high temperatures without melting or burning gives PBI a high degree of thermal stability [38]. These qualities make PBI resin perfect for several applications, such as support for polymer-supported catalysts, ion-exchange, separations, and purifications [15]. The PBI resin was refluxed with excess of $MoO_2(acac)_2$ in anhydrous toluene for a period of 4 days. The PBI.Mo catalyst particles were separated by filtration at the end of the reaction, and excess $MoO_2(acac)_2$ was removed by exhaustive extraction with acetone. It was observed that molybdenum in the produced catalysts was uniformly distributed throughout the polymer. The synthesis of polybenzimidazole-supported Mo(VI) (PBI.Mo) catalyst is shown in Figure 1.
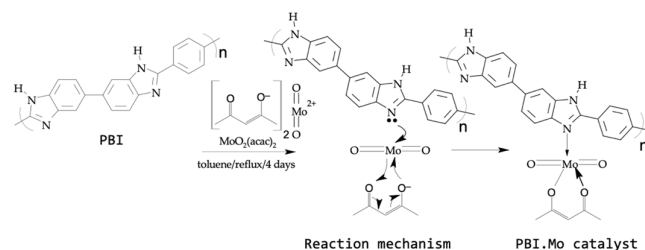

Figure 1. Reaction mechanism for the synthesis of polybenzimidazole-supported Mo(VI) (PBI.Mo) complex.

2.3. Characterisation of Polymer-Supported Mo(VI) Catalyst

The heterogeneous polybenzimidazole-supported Mo(VI) (PBI.Mo) catalyst was characterised to determine their molecular structure and morphological and physicochemical properties. The characterisation of the molecular structure included a Fourier transform infrared (FTIR) analysis. The morphological analysis of the catalyst was carried out using a scanning electron microscope (SEM). Brunauer–Emmett–Teller (BET)

surface area, pore volume, and pore diameter were determined the by nitrogen adsorption and desorption method using a Micromeritics Gemini VII. The particle size measurement was performed with a Malvern Mastersizer. An image of the prepared catalyst is shown in Figure 2.

Figure 2. Image of synthesised PBI.Mo catalyst.

2.3.1. Fourier Transform Infrared (FTIR) Spectroscopy Analysis

The FTIR spectrum of PBI.Mo catalyst was observed on a Thermal Nicolet Avectar 370 DTGS equipped(Thermo Electron) with a smart orbit accessory. A finely grounded sample of the catalyst was placed on the sample stage and the spectrum was recorded with the aid of OMINIC software. The PBI.Mo spectrum showed Mo=O and Mo-O-Mo vibrations characteristics with adsorption bonds around ~690 cm^{-1} to ~900 cm^{-1}. Hence, the FTIR spectrum of PBI.Mo catalyst confirms the incorporation of Mo centres in polymer resin due to the presence of Mo=O and Mo-O-Mo features, as shown in Figure 3.
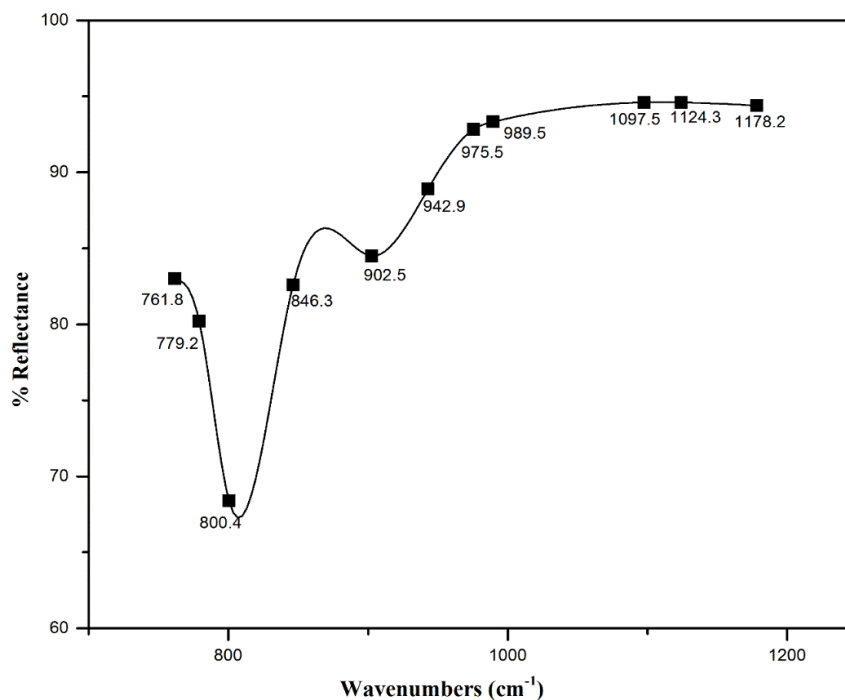

Figure 3. FTIR spectrum of PBI.Mo catalyst.

2.3.2. Determination of Molybdenum Content

The molybdenum content of the prepared catalysts was analysed using a PerkinElmer NexION 350D spectrophotometer(PerkinElmer, California, USA). Approximately 0.1 g of the sample was ground to fine powder and digested in 15 mL aqua regia for 3 days. Aqua regia is a mixture of concentrated HNO_3 and HCl in a ratio of 1:3. The mixture was diluted with distilled water to 100 mL, and Mo content was analysed using an ICP-mass spectrometer. The Mo content of PBI.Mo catalyst is given in Table 1.

Table 1. Properties of polybenzimidazole-supported Mo (i.e., PBI.Mo) catalyst.

Catalyst Properties	PBI.Mo Catalyst
BET surface area	18.44 m^2/g
Pore volume	0.021986 cm^3/g
Mo loading (mmol Mo g^{-1} resin)	0.825
Average pore diameter	21.595 Å
Average particle size	210–295 μm

2.3.3. Scanning Electron Microscopy (SEM)

The morphology of PBI.Mo catalyst particles was examined using a PEMTRON PS-230 scanning electron microscope(PEMTRON, Seoul, Korea). The catalyst was dried in a vacuum oven before analysing to remove any moisture present in the catalyst. Then the catalyst was mounted on the gold-coated specimen holder. The accelerating voltage for SEM analysis was set to ~8.0 Kv. The SEM image of the PBI.Mo catalyst, as shown in Figure 4, shows a well-dispersed spherical smooth surface. The SEM image of the catalyst shows negligible mechanical damage to the sample and shows that it has a well-dispersed spherical smooth surface, a property of macroporous polymeric resins [39].
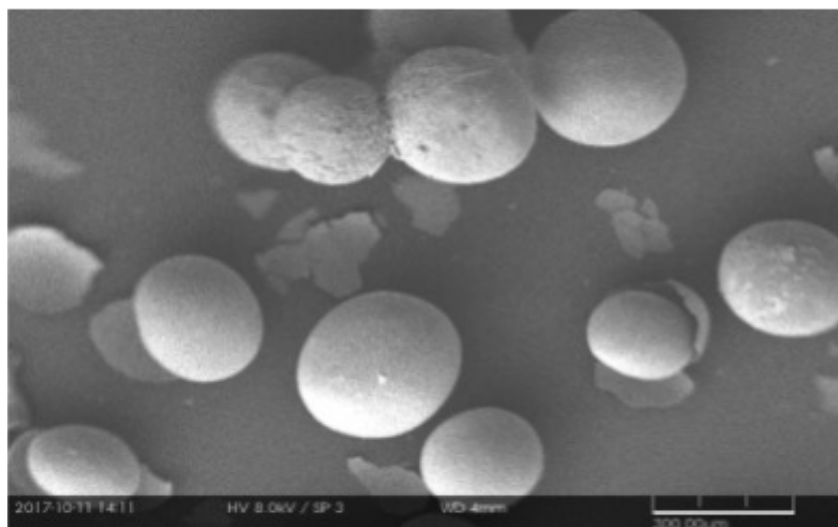

Figure 4. SEM image of PBI.Mo catalyst.

2.3.4. BET Surface Area, Pore Volume, and Pore Diameter Determination

The Brunauer–Emmett–Teller (BET) surface area, pore volume, and pore diameter were determined by the nitrogen adsorption and desorption method using a Micromeritics Gemini VII(Micromeritics at Norcross, Georgia). The instrument was fitted with a 133.3 Nm^{-2} pressure inducer. The weighed PBI.Mo sample was prepared by outgassing on the degassing port of the analyser. The temperature was kept at 373 K for 24 h. The adsorption isotherms were generated by dosing nitrogen onto the catalyst sample contained within a

bath of liquid nitrogen at ~77 K. The results for BET surface area, pore volume, and pore diameter of PBI.Mo are given in Table 1.

2.3.5. Average Particle Size Measurement

Particle size measurement was performed with a Malvern Mastersizer using the laser diffraction principle. A representative sample of the catalyst was initially moistened with demineralized water then stirred with a built-in agitator and recirculated around the loop. In particle size measurement, the experiment was repeated five times to achieve a reproducible result. As shown in Table 1, the PBI.Mo catalyst had particle sizes in the range of 210–295 μm.

2.4. Experimental Design

For analysing the relationships between variables and providing a quantitative illustration of how certain parameters impact responses, response surface methodology (RSM) is a powerful technique [40]. The Box–Behnken Design (BBD) method is one of the RSM techniques used to examine the significant effect of process factors on the response [41]. It also studies interactions between the factors to analyse the impact on the response [42]. The experimental runs were operated based on 4 independent variables, including reaction feed molar ratio of alkene to TBHP, reaction temperature, catalyst loading, and reaction time, which were labelled as A, B, C, and D, respectively. Three levels for each variable were coded as −1, 0, +1. The yield of 1,2-epoxy-5-hexene and 1,2-epoxy-7-octene was selected as the response for this study. The experiments were finished in a random order to reduce the impact of unexplained inconsistency in the response [43]. Design Expert 13 software (Stat-Ease Inc., Minneapolis, MN, USA) was used to identify and operate experimental design procedures. Twenty-nine runs were carried out randomly, and their responses were determined based on the outcomes of the experiment [44].

2.5. Statistical Analysis

To fit the experimental response with the independent variables, a model equation was developed [45]. The mathematical model was defined using the general quadratic model as shown in Equation (1).

$$Y = b_o + \sum_{i=1}^{n} b_i x_i + \sum_{i=1}^{n} b_{ii} x_i^2 + \sum_{i=1}^{n-1} \sum_{j>1}^{n} b_{ij}\, x_i x_j + \varepsilon \qquad (1)$$

where Y is the predicted response (i.e., the yield of 1,2-epoxy-7-octene); b_o is the model coefficient constant; b_i, b_{ii}, b_{ij}, are coefficients for the intercept of linear, quadratic, interactive terms, respectively; x_i, x_i are independent variables ($i \neq j$); n is several independent variables; and ε is the random error.

The adequacy of the predicted models was checked by several statistical validations including the coefficient of correlation (R^2), adjusted coefficient of determination (R^2_{adj}), and predicted coefficient of determination (R^2_{pred}). The statistical significance of the predicted models was analysed by ANOVA using Fisher's test, i.e., F-test, at a 95% confidence interval. The statistical significance of the results was presented by p-value, where the result is significant when the p-value is less than 0.05. Design Expert 13 software (Stat-Ease Inc., Minneapolis, MN, USA) was used to perform the initial experimental design, model prediction, statistical analysis, and optimisation.

2.6. Batch Epoxidation Studies

Using a polymer-supported Mo(VI) catalyst and TBHP as the oxidant, a 0.25 L jacketed four-neck glass reactor was used for the batch epoxidation of alkene. The batch

reactor's setup featured a condenser, overhead stirrer, digital thermocouple, sampling point, and water bath. The reactor vessel was filled with known amounts of alkene and TBHP, and the stirrer speed was adjusted to 400 rpm. The feed molar ratio (FMR) of alkene to TBHP of 2.5:1–10:1 was selected for charging the reactor. The temperature of the reaction mixture was allowed to reach the desired value, i.e., 333 K–353 K, and was maintained throughout the batch experiment. When the reaction reached the correct temperature, a known quantity of catalyst (0.15–0.6 mol% Mo loading) was added. The reaction scheme for the epoxidation of 1,5-hexadiene and 1,7-octadiene with TBHP is shown in Figure 5a and Figure 5b, respectively.

A sample was collected after the catalyst was added and the time was noted as zero time, i.e., t = 0. Subsequent samples were taken from the reaction mixture at specific time intervals and recorded. The samples collected were analysed using a Shimadzu GC-2014 gas chromatography (GC) instrument.
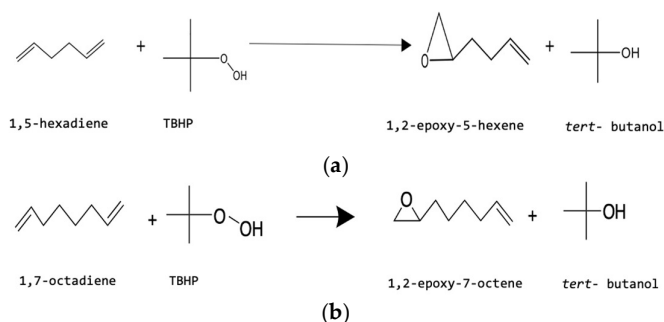

Figure 5. (**a**) Reaction scheme for epoxidation of 1,5-hexadiene with TBHP by PBI.Mo catalyst. (**b**) Reaction scheme for epoxidation of 1,7-octadiene with TBHP by PBI.Mo catalyst.

2.7. Method of Analysis

All the reactant and product compositions were analysed using a Shimadzu GC-2014 gas chromatography instrument after a specified quantity of internal standard (iso-octane) was added to the samples. The instrument had an auto-injector, a flame ionisation detector (FID), and a 30 m long Econo-CapTM-5 (ECTM-5) capillary column installed. Helium was used as a carrier gas, and the flow rate of carrier gas was 1 mLmin⁻¹. The split ratio was 100:1, and an injection volume of 0.5 μL was selected. The temperature for both the injector and detector was 523 K. Upon injection of the sample, the oven temperature was kept at 313 K for 4 min, and then it was gradually increased to 498 K at a rate of 20°C per minute. Each sample took ~13 min to be analysed by GC, and the temperature was cooled back to 313 K before starting the next run.

3. Results and Discussion

3.1. Development of Regression Model and Adequacy Checking

The response analysis utilising BBD was implemented following the completion of the 29 experiments and the assessment of the yield of 1,2-epoxy-5-hexene and 1,2-epoxy-7-octene (reaction responses) for each run. By fitting the experimental results, the generic quadratic equation shown in Equation (1) was used to obtain a model of polynomial regression. The polynomial equations for the epoxidation of 1,2-epoxy-5-hexene and 1,2-epoxy-7-octene are shown in Equations (2) and (3)**.**

$$Y = +53.27 - 2.50A + 1.45B + 4.44C + 9.17D - 2.81AB + 1.59AC - 0.1600AD$$
$$+ 1.86BC - 2.26BD + 0.5300CD + 1.63A^2 - 0.9042B^2 + 1.05C^2 \quad (2)$$
$$- 10.25D^2$$

$$Y = +52.29 + 3.64A + 5.40B + 2.56C + 27.76D + 0.8400AB + 2.63AC$$
$$+ 3.23AD + 0.6650BC + 2.56BD + 1.09CD - 5.27A^2 \qquad (3)$$
$$- 3.84B^2 - 3.15C^2 - 20.44D^2$$

where Y represents the dependent variable (yield of epoxide), while A, B, C, and D represent the independent variables, i.e., feed molar ratio, temperature, catalyst loading, and time, respectively. Further, AB, AC, AD, BC, BD, and CD represent the interaction between independent variables. Finally, A^2, B^2, C^2, and D^2 represent the excess of each independent variable.

The developed models demonstrated the effect of each independent variable, variable interactions, and excess of each variable on the response. Each variable's synergistic effect on the response is indicated by the positive sign of its coefficient. On the other hand, the negative sign denotes the response's antagonistic effect [46].

ANOVA was applied to examine the significance of the model parameters at a 95% confidence level. The significance of each parameter was determined by F-test and p-value. The higher the value of the F-test and the smaller the p-value, the more significant the corresponding parameter [47].

The model performance was observed using different techniques. A plot of the predicted versus experimental result of the yield of epoxides in Figure 6 showed a high correlation and reasonable agreement. In addition, a plot of residual distribution versus predicted response was presented to check the fitting performance of the model, as shown in Figure 7. Residual value is defined as the difference between predicted and experimental values of the response variable. The plot confirms that the quadratic model adequately represents the experimental data as the distribution does not follow a specified trend with respect to the predicted values of the response variable. Moreover, the perturbation plot represents the effect of each variable on the reaction response as shown in Figure 8. The curvature of the variables from the centre point indicates the significance of each variable, which confirms the statistical results obtained from ANOVA as shown in Tables 2 and 3.
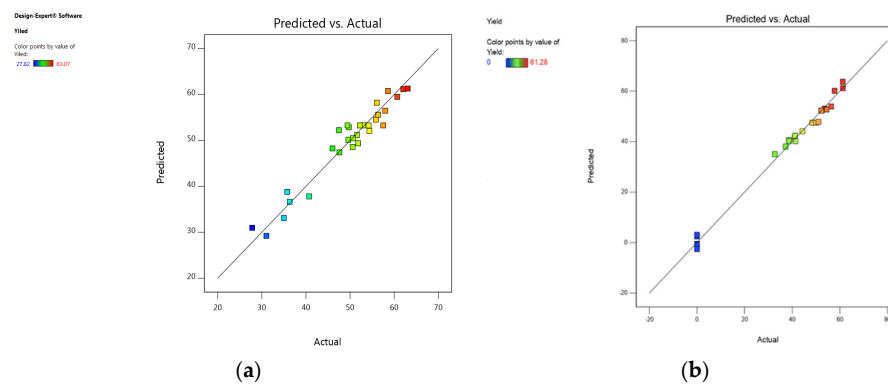

Figure 6. Actual experimental data versus predicted model of the yield of epoxide: (**a**) 1,2-epoxy-5-hexene, (**b**) 1,2-epoxy-7-octene.
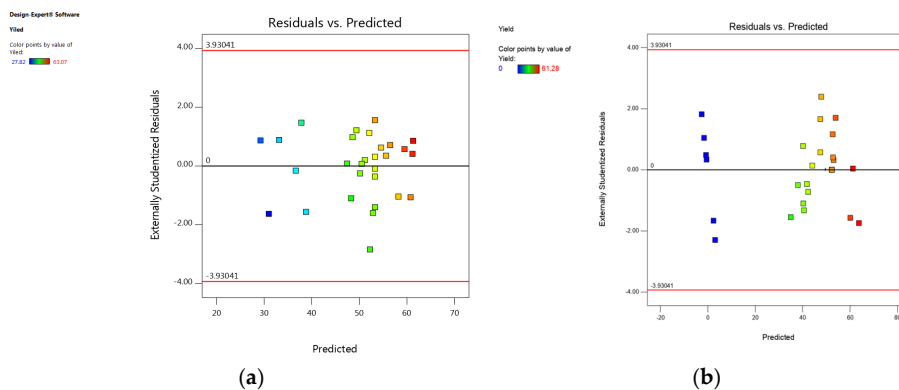
Figure 7. Residual versus predicted response: (**a**) 1,2-epoxy-5-hexene, (**b**) 1,2-epoxy-7-octene.
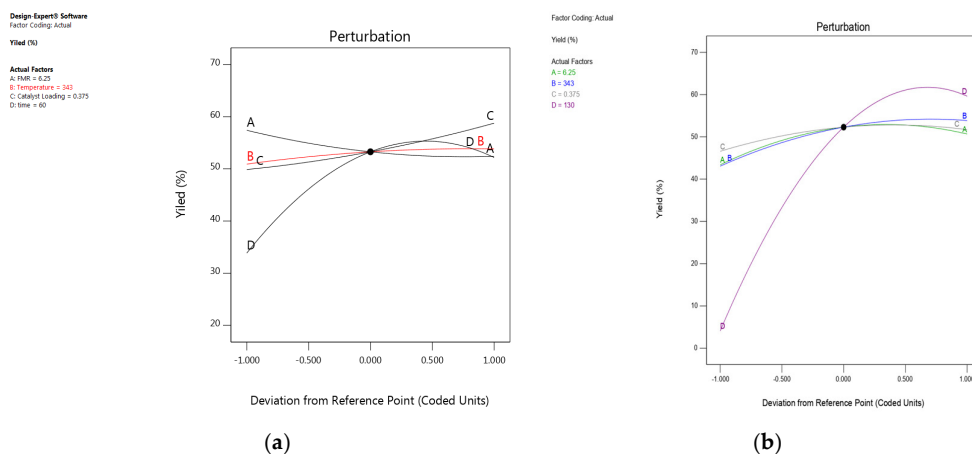

Figure 8. The perturbation plot represents the effect of each variable on the reaction response: (**a**) 1,2-epoxy-5-hexene, (**b**) 1,2-epoxy-7-octene.

Table 2. Analysis of variance for response surface developed model for the epoxidation of 1,5-hexadiene.

Source	Sum of Squares	df	Mean Square	F-Value	*p*-Value	Significance
Model	2230.55	14	159.33	15.69	<0.0001	Significant
A-FMR	75.00	1	75.00	7.39	0.0167	Significant
B-Temperature	25.35	1	25.35	2.50	0.1364	Not significant
C-Catalyst loading	236.47	1	236.47	23.29	0.0003	Significant
D-Time	1008.52	1	1008.52	99.34	<0.0001	Significant
AB	31.58	1	31.58	3.11	0.0996	Not significant
AC	10.18	1	10.18	1.00	0.3337	Not significant
AD	0.1024	1	0.1024	0.0101	0.9214	Not significant
BC	13.80	1	13.80	1.36	0.2631	Not significant
BD	20.39	1	20.39	2.01	0.1783	Not significant
CD	1.12	1	1.12	0.1107	0.7443	Not significant
A^2	17.20	1	17.20	1.69	0.2141	Not significant
B^2	5.30	1	5.30	0.5223	0.4817	Not significant
C^2	7.11	1	7.11	0.7005	0.4167	Not significant
D^2	681.87	1	681.87	67.17	<0.0001	Significant
Residual	142.13	14	10.15			
Lack of fit	107.22	10	10.72	1.23	0.4557	Not significant
Pure error	34.91	4	8.73			
Cor total	2372.68	28				

Table 3. Analysis of variance for response surface developed model for the epoxidation of 1,7-octa-diene.

Source	Sum of Squares	df	Mean Square	F-Value	*p*-Value	Significance
Model	12,671.98	14	905.14	159.75	<0.0001	Significant
A-FMR	159.21	1	159.21	28.10	0.0001	Significant
B-Temperature	349.38	1	349.38	61.66	<0.0001	Very significant
C-Catalyst loading	78.69	1	78.69	13.89	0.0023	Significant
D-Time	9250.19	1	9250.19	1632.59	<0.0001	Very significant
AB	2.82	1	2.82	0.4981	0.4919	Not significant
AC	27.62	1	27.62	4.87	0.0445	Significant
AD	41.60	1	41.60	7.34	0.0169	Significant
BC	1.77	1	1.77	0.3122	0.5852	Not significant
BD	26.16	1	26.16	4.62	0.0496	Significant
CD	4.75	1	4.75	0.8388	0.3753	Not significant
A2	180.06	1	180.06	31.78	<0.0001	Very significant
B2	95.46	1	95.46	16.85	0.0011	Significant
C2	64.31	1	64.31	11.35	0.0046	Significant
D2	2710.34	1	2710.34	478.36	<0.0001	Very significant
Residual	79.32	14	5.67			
Lack of fit	79.32	10	7.93			
Pure error	0.0000	4	0.0000			
Cor total	12,751.31	28				

3.2. Effect of Process Variables and Their Interactions

The effect of each independent process variable on the process response is investigated in this section. In addition, the interactive effect is highlighted on the response of various independent variables. Three-dimensional response surface plots were created for a model equation after constructing the regression model and evaluating the model adequacy. The 3D surface plots of the interaction between epoxide yield versus two independent variables are displayed. The two remaining independent variables are kept constant in their centre points in each plot. Three-dimensional response surfaces help in understanding system behaviour. Additionally, they help in identifying the reaction surface's characters [48,49].

3.2.1. Effect of Feed Molar Ratio (FMR)

The ANOVA results provide strong evidence that raising the feed mole ratio (FMR) of the alkenes to TBHP speeds up the desired epoxides' synthesis. We changed the feed molar ratio of alkene to TBHP between 2.5:1 and 10:1 to examine the effect of the feed molar ratio on epoxide production. Figure 9 demonstrates that the rate of production of 1,2-epoxy-7-octene increased steadily from 43.38% to 53% as the feed molar ratio increased from 2.5:1 to 7.6:1. However, when the FMR of an alkene to TBHP is raised from 7.85:1 to 10:1, production of 1,2-epoxy-7-octene formation is slowed. The influence of FMR of 1,5-hexadiene to TBHP was more noticeable when a stoichiometric ratio (2.5:1) was used, as there was no significant difference in the rate of epoxidation when the feed molar ratio of 1,5-hexadiene to TBHP was increased from 2.5:1 to 10:1. Figure 9 suggests that alkene concentration affects the epoxidation of alkenes using a PBI catalyst [15]. Amborziak et al. mentioned that increasing the feed molar ratio lowers the TBHP concentration to such an extent that it slows down the conversion of TBHP into epoxide [50]. A similar feed molar ratio effect was reported in my previously published results [51]. According to

the result of this study, at 348 K temperature and 0.56 mol% catalyst loading, the optimum molar feed ratio of 1,5-hexadiene to TBHP was 2.76:1 at 76 min. According to the 3D surface plot, the maximum epoxide yield (67.24%) was obtained at a reaction time of 218 min and a feed molar ratio of 8.5:1, showing that increasing the reaction time from 0 min to 218 min increases the yield of 1,2-epoxy-7-octene, as shown in Figure 10.
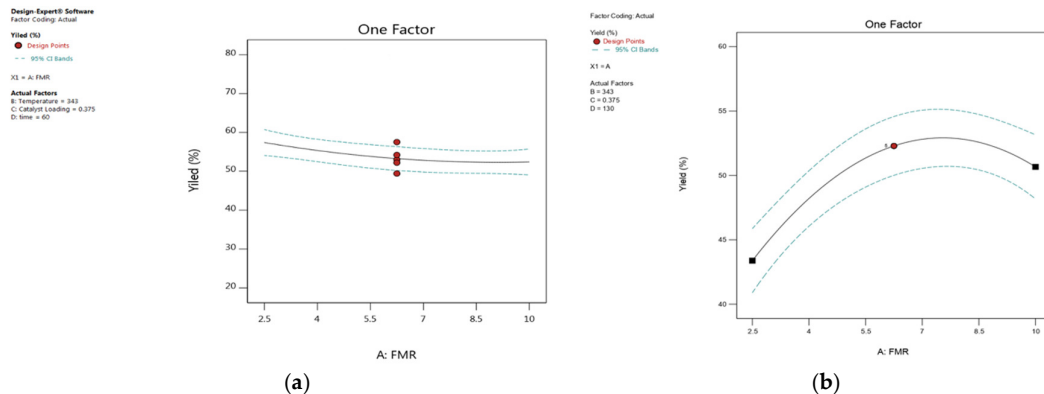

(**a**)

(**b**)

Figure 9. The plot shows the effect of feed molar ratio on percentage yield: (**a**) 1,2-epoxy-5-hexene, (**b**) 1,2-epoxy-7-octene.
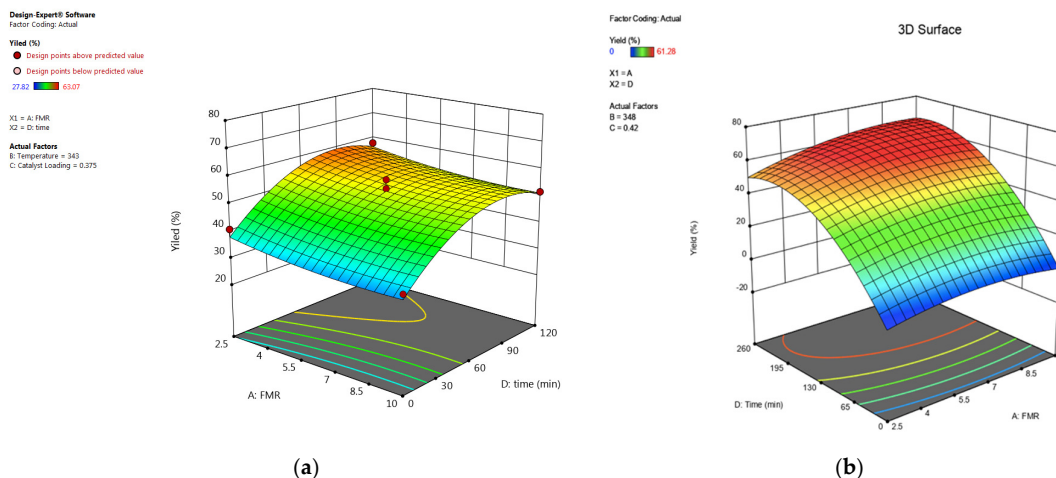

(**a**)

(**b**)

Figure 10. Three-dimensional response surface of the effect of feed molar ratio and time on percentage yield: (**a**) 1,2-epoxy-5-hexene, (**b**) 1,2-epoxy-7-octene.

3.2.2. Effect of Reaction Temperature

The epoxidation of 1,5-hexadiene and 1,7-octadiene with TBHP was carried out at 333 K, 343 K, and 353 K to study the effect of reaction temperature on the yield of epoxides. The ANOVA results of the epoxidation of 1,5-hexadiene presented in Table 2 show no significant effect of reaction temperature on the process response, but the ANOVA results of the epoxidation of 1,7-octadiene show there is a very significant effect of reaction temperature on the process response. Figure 11 shows that when temperature increased from 333 K to 343 K, the yield of 1,2-epoxy-7-octene increased consistently from 43.06% to 52.29%, which is a directly proportional relationship between temperature and epoxide yield. However, at higher temperature values above 353 K, a progressive decline in yield was recorded. Mohammed et al. [15] reported similar results for the epoxidation of 1-hexene with TBHP in the presence of PBI.Mo catalyst. It is clearly shown in Figure 12 that at 60 min, the yield of 1,2-epoxy-5-hexene was 54.25% and 57.1% at 333 K and 353 K, respectively. The 3D surface graph (Figure 12) shows that the yield of 1,2-epoxy-5-hexene

at 0.35 mol% catalyst loading was 50.73% and 53.23% at 333 K and 353 K, respectively. This was due to a distinct exothermic effect. Mohammed et al. [52] reported a similar result for the epoxidation of 4-vinyl-1-cyclohexene with TBHP where the reaction reached equilibrium within the first 5 min. It can be concluded that at 0.56 mol% catalyst loading, 348 K is the preferred reaction temperature for the epoxidation of 1,5-hexadiene at 76 min, and the feed molar ratio of 1,5-hexadiene to TBHP is 2.76:1. The 3D surface plot revealed that the yield of epoxide was 67.07% at a reaction time of 218 min and temperature of 348 K, suggesting that raising the reaction temperature from 333 K to 348 K increases epoxide yield, as shown in Figure 12.
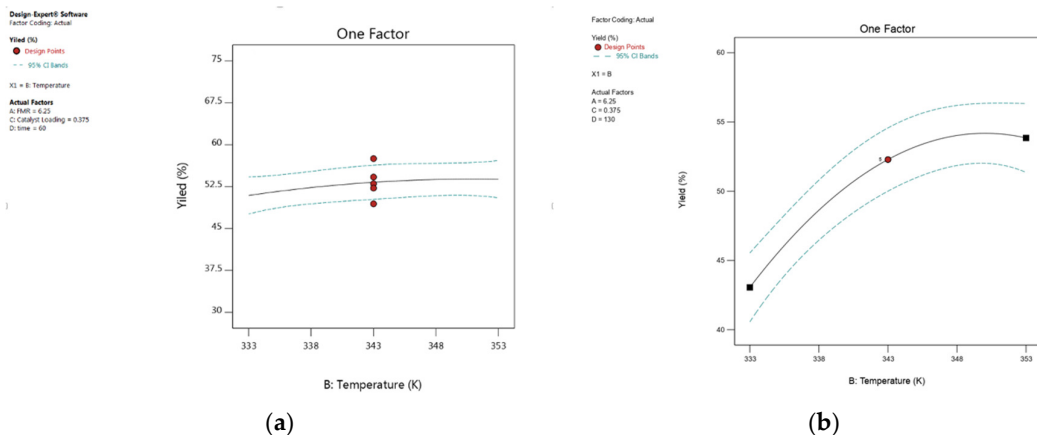

(**a**) (**b**)

Figure 11. The plot shows the effect of temperature on percentage yield: (**a**) 1,2-epoxy-5-hexene, (**b**) 1,2-epoxy-7-octene.
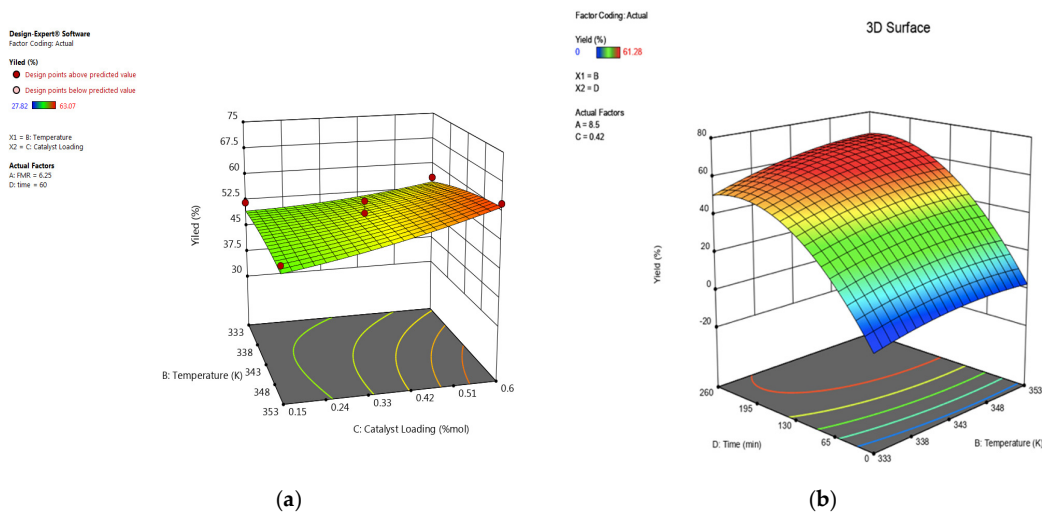

(**a**) (**b**)

Figure 12. (**a**) Three-dimensional response surface of the effect of temperature and catalyst loading on percentage yield of 1,2-epoxy-5-hexene. (**b**) Three-dimensional response surface of the effect of temperature and time on percentage yield of 1,2-epoxy-7-octene.

3.2.3. Effect of Catalyst Loading

Catalyst loading is described in this study as a percentage of the mole ratio of Mo to TBHP. In this research, a single batch of the produced catalysts was used for batch investigations. The effect of catalyst loading for epoxidation with TBHP was investigated by conducting batch experiments using 0.15 mol% Mo, 0.375 mol% Mo, and 0.6 mol% Mo catalyst loading. Based on the ANOVA results presented in Tables 2 and 3, the catalyst loading parameter shows a significant effect on the process response. As shown in Figure

13, it can be observed that the yield of 1,2-epoxy-7-octene increased along with the increase in catalyst loading, from 46.58% to a maximum of 52.87% at 0.45 mol% Mo catalyst loading. It gradually declined once the catalyst loading was increased to 0.6 mol%, demonstrating that the optimum catalyst loading was reached. Figure 13 also shows that a positive correlation exists between catalyst loading and the yield of 1,2-epoxy-5-hexene within the temperature range between 333 K and 353 K. The yield of 1,2-epoxy-5-hexene at 60 min was ~49% and ~59% for reactions conducted at 0.15 mol% Mo and 0.6 mol% Mo, respectively, while the FMR of 1,5-hexadiene to TBHP was 6.25:1. For example, Figure 14 shows that at a lower catalyst loading of 0.15 mol% Mo, only 48% of epoxide yield was recorded because of low 1,7-octadiene conversion at low catalyst loading. The epoxide yield increased steadily up to 67% as the feed molar ratio increased at moderate levels of catalyst loading from 0.15 mol% to 0.42 mol%. This phenomenon may be explained by an increase in the catalyst's surface area, which increases the surface area available for contact between the catalyst's active sites and the reactant, 1,7-octadiene [53]. The increase in catalyst loading from 0.15 mol% Mo to 0.42 mol% enhances the epoxide yield from 48% to 53.1% for lower feed molar ratios (for example, at 2.5:1). As seen in Figure 14, the yield of 1,2-epoxy-7-octene increases proportionally with catalyst loading at any designated value between 0.15 mol% and 0.42 mol%. A low p-value (0.0023) also provided support for this observation. Figure 14 shows that the yield of 1,2-epoxy-5-hexene at a feed molar ratio of 1,5-hexadiene to TBHP of 9.6:1 was ~47% and ~57% at 0.15 mol% Mo and 0.5 mol% Mo, respectively. It can be concluded that 0.56 mol% catalyst loading is the preferred catalyst loading at 348 K for the epoxidation of 1,5-hexadiene at 76 min, and the feed molar ratio of 1,5-hexadiene to TBHP is 2.76:1.
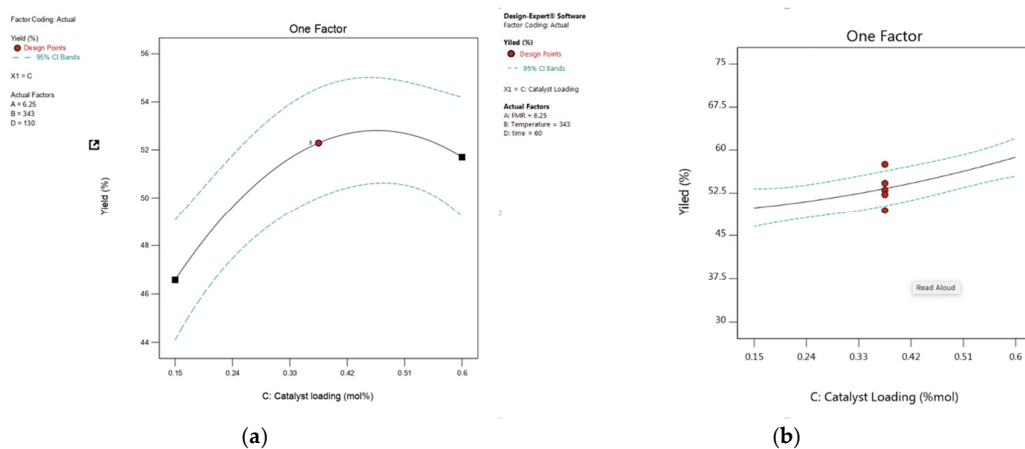

(**a**)   (**b**)

Figure 13. The plot shows the effect of catalyst loading on percentage yield: (**a**) 1,2-epoxy-7-octene, (**b**) 1,2-epoxy-5-hexene.
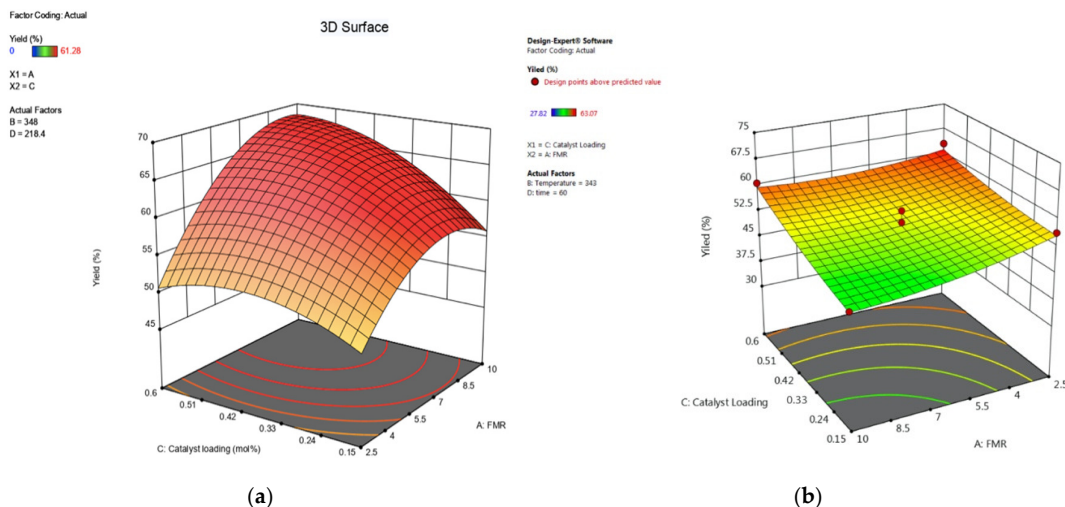
Figure 14. Three-dimensional response surface of the effect of catalyst loading and feed molar ratio on percentage yield: (**a**) 1,2-epoxy-7-octene, (**b**) 1,2-epoxy-5-hexene.

3.2.4. Effect of Reaction Time

In this investigation, the catalyst was introduced, and the reaction time was recorded as zero time, or $t = 0$. At certain intervals, samples were obtained from the reaction mixture again and recorded. The reaction time parameter has a highly significant impact on the process response, according to the ANOVA results shown in Tables 2 and 3. The result shows a fairly large increase in the rate of epoxidation with an increase in time. As shown in Figure 15, the yield of 1,2-epoxy-5-hexene increases by increasing the time between 0 min and 87 min. Figure 15 also shows that at 343 K, the yield of 1.2-epoxy-5-hexene was 30% and 58% at 0 min and 80 min, respectively. The yield of epoxide starts to decrease after 87 min. The 3D surface graph (Figure 16) shows that the yield of epoxide at 0.4 mol% catalyst loading was 40%, 56%, and 53% at 12 min, 88 min, and 118 min, respectively. It can be concluded that 76 min is the preferred reaction time at 348 K for the epoxidation of 1,5-hexadiene at 0.56 mol% catalyst loading, and the feed molar ratio of 1,5-hexadiene to TBHP is 2.76:1. As seen in Figure 15, the yield of 1,2-epoxy-7-octene increased gradually as reaction time increased until it reached 60.4% in 218 min. After 218 min, epoxide production decreased even more as reaction time was extended. A similar phenomenon was reported when PBI.Mo catalysed the epoxidation of 1-hexene and 4-vinyl-1-cyclohexene with TBHP, where an increase in reaction time from 0 to 260 min was directly proportional to the corresponding epoxide yield [15]. Figure 16 shows that increasing the feed molar ratio from 2.5:1 to 8.5:1 resulted in yields of 1,2-epoxy-7-octene of 52.9% and 67.24%, respectively, after 218 min of reaction time. However, when the 1,7-octadiene-to-TBHP feed molar ratio was larger than 8.5:1 and the reaction time was greater than 218 min, the percentage yield of epoxidation did not change significantly. According to the 3D surface plot, the maximum epoxide yield (67.24%) was obtained at a reaction time of 218 min and a feed molar ratio of 8.5:1, showing that increasing the reaction time from 0 min to 218 min increased the yield of 1,2-epoxy-7-octene, as shown in Figure 16. The results demonstrate a rise in the epoxidation rate with increasing time. However, an increase in feed molar ratio of 1,7-octadiene to TBHP beyond 8.5:1 at 218 min of reaction time was unfavourable to the reactive system, causing a marginal drop in epoxide yield from 67.24% to 66.66%. It can be concluded from the ANOVA in Table 3 that the reaction time was found to be a highly influencing parameter on epoxide yield as evidenced by a low *p*-value (<0.0001).
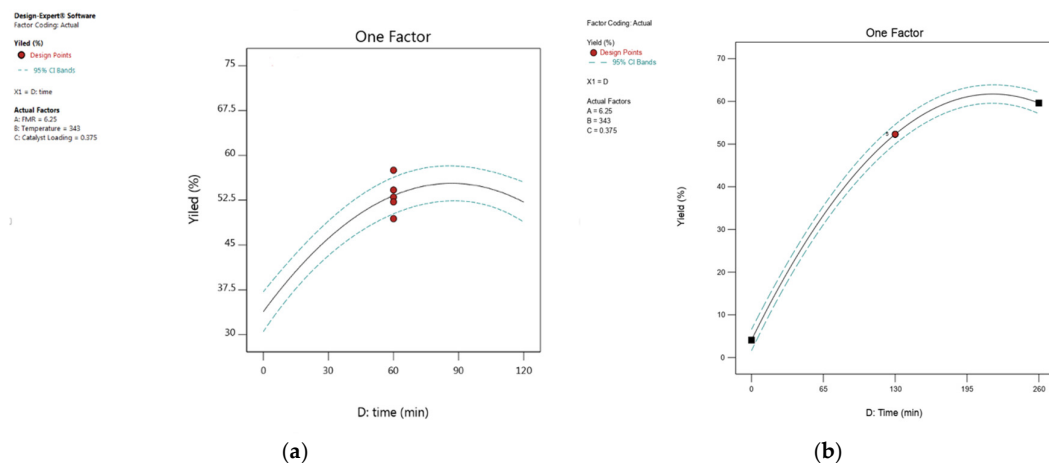
(**a**)   (**b**)

Figure 15. The plot shows the effect of reaction time on percentage yield: (**a**) 1,2-epoxy-5-hexene, (**b**) 1,2-epoxy-7-octene.

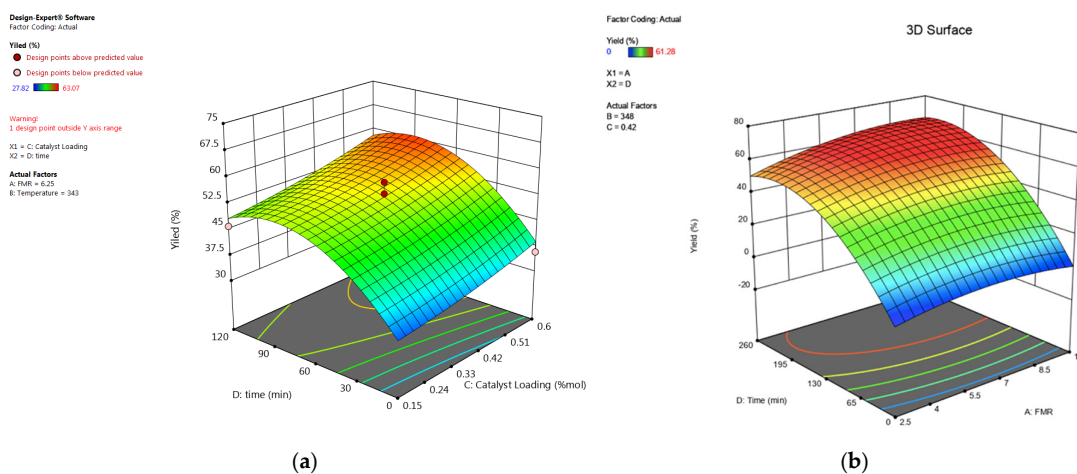(**a**)   (**b**)

Figure 16. (**a**) Three-dimensional response surface of the effect of time and catalyst loading on percentage yield of 1,2-epoxy-5-hexene. (**b**) Three-dimensional response surface of the effect of time and feed molar ratio on percentage yield of 1,2-epoxy-7-octene.

3.3. Optimisation Study of Reaction Variables

It is very straightforward to use RSM to find the optimal reaction parameters for a single response, but it might be more challenging to optimise multiple responses [53]. To determine the optimum values for the independent factors affecting the dependent response variable, an optimisation approach to the epoxidation reaction was conducted. The numerical optimisation stage was developed using Design Expert software, which combined the desirability of each independent variable into a single value and then looked for the response objectives' optimal values. As a result, a set of goals must be entered into the program to direct the optimisation process to determine the optimal conditions for the independent variables [47].

The reaction temperature and time were both set at minimal values to minimise production cost at a maximum economic benefit, while the dependent response variable, which is the yield of 1,2-epoxy-5-hexene and 1,2-epoxy-7-octene, was set to be maximised to obtain the maximum yield [51,54]. No specific target for catalyst loading was established due to the catalyst's stability and efficiency at optimal conditions. The numerical optimisation technique concluded that the maximum yield of 1,2-epoxy-5-hexene can be reached is 64.2% at a feed molar ratio of 2.76:1, a reaction temperature of 348 K, a 0.56

mol% catalyst loading, and a reaction time of 76 min. The numerical optimisation technique also concluded that the maximum yield of 1,2-epoxy-7-octene can be reached is 66.22% at a feed molar ratio of 7.97:1, reaction temperature 347 K, 0.417 mol% catalyst loading, and reaction time of 218 min.

3.4. Optimum Conditions Validation

To validate the optimal response values of the predicted quadratic equation, experiments were performed at optimum conditions. The experimental results of the epoxidation of 1,5-hexadiene showed a similar response value to the predicted optimal response of 62.03% with a relative error of 3.5%. The experimental results of the epoxidation of 1,7-octadiene showed a similar response value to the predicted optimal response of 64.97% with a relative error of 1.92%. The relative error can be affected by the temperature variation of the reaction.

4. Conclusions

Polymer-supported Mo(VI) (PBI.Mo complex) was prepared and characterised. The performance of the catalyst was evaluated for the epoxidation of 1,5-hexadiene and 1,7-octadiene using TBHP as an oxidant. In this epoxidation process, Design Expert 13 software (Stat-Ease Inc., Minneapolis, MN, USA) was used to identify and operate the batch experimental design procedures. The Box–Behnken Design (BBD) method is one of the RSM techniques that was used to examine the significant effect of various factors on epoxides. The optimum conditions that were observed for the maximum yield of 1,2-epoxy-5 hexene are 2.76:1 molar feed ratio, 348 K reaction temperature, 76 min reaction time, and 0.56 mol% catalyst loading. The optimal conditions for achieving the maximum yield of 1,2-epoxy-7-octene were determined to be a molar feed ratio of alkene to TBHP of 7.97:1, a reaction temperature of 347 K, a reaction time of 218 min, and a catalyst loading of 0.417 mol%. These optimised conditions were experimentally validated, confirming the accuracy of the predicted results.

PBI.Mo catalyst was proven to be highly active for both epoxidation reactions. The results of this work demonstrate the feasibility of creating polymer-supported Mo catalysts for alkene epoxidation. The batch experimental work demonstrated the effectiveness of polymer-supported catalysts in the epoxidation of both alkenes studied. In the use of PBI.Mo as the catalyst, 1,5-hexadiene exhibits the highest reaction rate. This study highlights that polymer-supported Mo(VI) (PBI.Mo complex) is an effective catalyst for a greener and more efficient epoxidation process, using *tert*-butyl hydroperoxide (TBHP) as the oxidising agent to produce two important epoxides -1,2-epoxy-5 hexene and 1,2-epoxy-7-octene. The results obtained from this study provide useful information for conducting continuous epoxidation experiments.

Author Contributions: M.M.R.B.: methodology, software, validation, visualisation, formal analysis, data curation, writing—original draft preparation; B.S.: conceptualisation, writing—review and editing, formal analysis, data curation, resources, supervision, funding acquisition, and project administration. All authors have read and agreed to the published version of the manuscript.

Data Availability Statement: The data will be made available upon request.

Conflicts of interest: There are no conflicts to declare.

References

1. Haag, R.; Roller, S. Polymeric Supports for the Immobilisation of Catalysts. In *Immobilized Catalysts*; Kirschning, A., Ed.; Springer: Berlin/Heidelberg, Germany, 2004; Volume 242, pp. 1–42.

2. Leadbeater, N.E.; Marco, M. Preparation of Polymer-Supported Ligands and Metal Complexes for Use in Catalysis. *Chem. Rev.* **2002**, *102*, 3217–3274.

3. Clapham, B.; Reger, T.S.; Janda, K.D. Polymer-supported catalysis in synthetic organic chemistry. *Tetrahedron* **2001**, *57*, 4637–4662.

4. Sherrington, D.C. Polymer-supported reagents, catalysts, and sorbents: Evolution and exploitation—A personalized view. *J. Polym. Sci. A Polym. Chem.* **2001**, *39*, 2364–2377.

5. Shen, Y.; Jiang, P.; Zhang, J.; Bian, G.; Zhang, P.; Dong, Y.; Zhang, W. Highly dispersed molybdenum incorporated hollow mesoporous silica spheres as an efficient catalyst on epoxidation of olefins. *Mol. Catal.* **2017**, *433*, 212–223.

6. Bisio, C.; Gallo, A.; Psaro, R.; Tiozzo, C.; Guidotti, M.; Carniato, F. Tungstenocene-grafted silica catalysts for the selective epoxidation of alkenes. *Appl. Catal. A Gen.* **2019**, *581*, 133–142.

7. Cai, L.; Chen, C.; Wang, W.; Gao, X.; Kuang, X.; Jiang, Y.; Li, L.; Wu, G. Acid-free epoxidation of soybean oil with hydrogen peroxide to epoxidized soybean oil over titanium silicalite-1 zeolite supported cadmium catalysts. *J. Ind. Eng. Chem.* **2020**, *91*, 191–200.

8. Wu, Z.; He, Z.; Zhou, D.; Yang, Y.; Lu, X.; Xia, Q. One-step synthesis of bi-functional zeolite catalyst with highly exposed octahedral Co for efficient epoxidation of bulky cycloalkenes. *Mater. Lett.* **2020**, *280*, 128549.

9. Lueangchaichaweng, W.; Singh, B.; Mandelli, D.; Carvalho, W.A.; Fiorilli, S.; Pescarmona, P.P. High surface area, nanostructured boehmite and alumina catalysts: Synthesis and application in the sustainable epoxidation of alkenes. *Appl. Catal. A Gen.* **2019**, *571*, 180–187.

10. Mikolajska, E.; Calvino-Casilda, V.; Bañares, M.A. Real-time Raman monitoring of liquid-phase cyclohexene epoxidation over alumina-supported vanadium and phosphorous catalysts. *Appl. Catal. A Gen.* **2012**, *421–422*, 164–171.

11. Borugadda, V.B.; Goud, V.V. Epoxidation of Castor Oil Fatty Acid Methyl Esters (COFAME) as a Lubricant base Stock Using Heterogeneous Ion-exchange Resin (IR-120) as a Catalyst. *Energy Proced.* **2014**, *54*, 75–84.

12. Peng, C.; Lu, X.H.; Ma, X.T.; Shen, Y.; Wei, C.C.; He, J.; Zhou, D.; Xia, Q.H. Highly efficient epoxidation of cyclohexene with aqueous H_2O_2 over powdered anion-resin supported solid catalysts. *J. Mol. Catal. A-Chem.* **2016**, *423*, 393–399.

13. Otake, K.; Ahn, S.; Knapp, J.; Hupp, J.T.; Notestein, J.M.; Farha, O.K. Vapor-Phase Cyclohexene Epoxidation by Single-Ion Fe(III) Sites in Metal–Organic Frameworks. *Inorg. Chem.* **2021**, *60*, 2457–2463.

14. Zhao, Q.; Bai, C.; Zhang, W.; Li, Y.; Zhang, G.; Zhang, F.; Fan, X. Catalytic Epoxidation of Olefins with Graphene Oxide Supported Copper (Salen) Complex. *Ind. Eng. Chem. Res.* **2014**, *53*, 4232–4238.

15. Mohammed, M.L.; Patel, D.; Mbeleck, R.; Niyogi, D.; Sherrington, D.C.; Saha, B. Optimisation of alkene epoxidation catalysed by polymer supported Mo(VI) complexes and application of artificial neural network for the prediction of catalytic performances. *Appl. Catal. A-Gen.* **2013**, *466*, 142–152.

16. Tada, M.; Muratsugu, S.; Kinoshita, M.; Sasaki, T.; Iwasawa, Y. Alternative selective oxidation pathways for aldehyde oxidation and alkene epoxidation on a SiO_2-supported Ru-monomer complex catalyst. *J. Am. Chem. Soc.* **2010**, *132*, 713–724.

17. Sharma, A.S.; Sharma, V.S.; Kaur, H.; Varma, R.S. Supported heterogeneous nanocatalysts in sustainable, selective and eco-friendly epoxidation of olefins. *Green Chem.* **2020**, *22*, 5902–5936.

18. Mohammed, M.L.; Saha, B. Greener and sustainable approach for the synthesis of commercially important epoxide building blocks using polymer-supported Mo(VI) complexes as catalysts. In *Ion Exchange and Solvent Extraction*, 1st ed.; SenGupta, A.K., Ed.; CRC Press: Boca Raton, FL, USA; Taylor & Francis Group LLC.: Milton Park, UK, 2016; p. 33.

19. Gupta, K.C.; Sutar, A.K.; Lin, C.C. Polymer-supported Schiff base complexes in oxidation reactions. *Coord. Chem. Rev.* **2009**, *253*, 1926–1946.

20. Mbeleck, R.; Mohammed, M.L.; Ambroziak, K.; Sherrington, D.C.; Saha, B. Efficient epoxidation of cyclododecene and dodecene catalysed by polybenzimidazole supported Mo(VI) complex. *Catal. Today* **2015**, *256*, 287–293.

21. Mohammed, M.L.; Saha, B. Recent Advances in Greener and Energy Efficient Alkene Epoxidation Processes. *Energies* **2022**, *15*, 2858.

22. Mbeleck, R.; Ambroziak, K.; Saha, B.; Sherrington, D.C. Stability and recycling of polymer-supported Mo(VI) alkene epoxidation catalysts. *React. Funct. Polym.* **2007**, *67*, 1448–1457.

23. Schaus, S.E.; Brandes, B.D.; Larrow, J.F.; Tokunaga, M.; Hansen, K.B.; Gould, A.E.; Furrow, M.E.; Jacobsen, E.N. Highly Selective Hydrolytic Kinetic Resolution of Terminal Epoxides Catalyzed by Chiral (salen)CoIII Complexes. Practical Synthesis of Enantioenriched Terminal Epoxides and 1,2-Diols. *J. Am. Chem. Soc.* **2002**, *124*, 1307–1315.

24. Grivani, G.; Tangestaninejad, S.; Habibi, M.H.; Mirkhani, V. Epoxidation of alkenes by a highly reusable and efficient polymer-supported molybdenum carbonyl catalyst. *Catal. Commun.* **2005**, *6*, 375–378.

25. Grivani, G.; Tangestaninejad, S.; Habibi, M.H.; Mirkhani, V.; Moghadam, M. Epoxidation of alkenes by a readily prepared and highly active and reusable heterogeneous molybdenum-based catalyst. *Appl. Catal. A Gen.* **2006**, *299*, 131–136.

26. Yahya, S.N.; Lin, C.K.; Ramli, M.R.; Jaafar, M.; Ahmad, Z. Effect of cross-link density on optoelectronic properties of thermally cured. *Mater. Des.* **2013**, *47*, 416–423.

27. Bader, R.A. Synthesis and viscoelastic characterization of novel hydrogels generated via photopolymerization of 1,2-epoxy-5-hexene modified poly(vinyl alcohol) for use in tissue replacement. *Acta Biomater.* **2008**, *4*, 967–975.

28. García, R.; Martínez, M.; Aracil, J. Enzymatic esterification of an acid with an epoxide using immobilized lipase from Mucor miehei as catalyst: Optimization of the yield and isomeric excess of ester by statistical analysis. *J. Ind. Microbiol. Biotechnol.* **2002**, *28*, 173–179.

29. Allgaier, J.; Hövelmann, C.H.; Wei, Z.; Staropoli, M.; Pyckhout-Hintzen, W.; Lühmann, N.; Willbold, S. Synthesis and rheological behavior of poly(1,2-butylene oxide) based supramolecular architectures. *RSC Adv.* **2016**, *6*, 6093–6106.

30. Bian, F.; Lin, S. Preparation of epoxy-based silicone prepolymers with applications in UV-curable coatings. *Pigment. Resin Technol.* **2024**, *53*, 650–658.

31. Tzevi, R.; Novakov, P.; Troev, K.; Roundhill, D.M. Synthesis of poly (oxyethylene phosphonate) s bearing oxirane groups in the side chain. *J. Polym. Sci. A Polym. Chem.* **1997**, *35*, 625–630.

32. Santacesaria, E.; Tesser, R.; Di Serio, M.; Turco, R.; Russo, V.; Verde, D. A biphasic model describing soybean oil epoxidation with H_2O_2 in a fed-batch reactor. *Chem. Eng. J.* **2011**, *173*, 198–209.

33. The Many Uses and Hazards of Peracetic Acid. Available online: https://synergist.aiha.org/201612-peracetic-acid-uses-and-hazards, (accessed on 12 July 2023).

34. Kollar, J. Epoxidation Process. U.S. Patent Number US53617966A, 11 July 1967.

35. Salavati-Niasari, M.; Esmaeili, E.; Seyghalkar, H.; Bazarganipour, M. Cobalt(II) Schiff base complex on multi-wall carbon nanotubes (MWNTs) by covalently grafted method: Synthesis, characterization and liquid phase epoxidation of cyclohexene by air. *Inorg. Chim. Acta* **2011**, *375*, 11–19.

36. Patel, D.; Kellici, S.; Saha, B. Green process engineering as the key to future processes. *Processes* **2014**, *2*, 311–332.

37. Mohammed, M.L.; Mbeleck, R.; Saha, B. Efficient and selective molybdenum based heterogeneous catalyst for alkene epoxidation using batch and continuous reactors. *Polym. Chem.* **2015**, *6*, 7308–7319.

38. Paglia, L.; Genova, V.; Bracciale, M.P.; Bartili, C.; Marra, F.; Natali, M.; Pulci, G. Thermochemical characterization of polybenzimidazole with and without nano-ZrO_2 for ablative materials application. *J. Therm. Anal. Calorim.* **2020**, *142*, 2149–2161.

39. Leinonen, S.; Sherrington, D.C.; Sneddon, A.; Mcloughlin, D.; Corker, J.; Canevali, C.; Morazzoni, F.; Reedijk, J.; Spratt, S.B.D. Molecular Structural and Morphological Characterization of Polymer-Supported Mo (V) Alkene Epoxidation Catalysts. *J. Catal.* **1999**, *2*, 251–266.

40. Yuan, J.; Huang, J.; Wu, G.; Tong, J.; Xie, G.-Y.; Duan, J.-a.; Qin, M. Multiple responses optimization of ultrasonic-assisted extraction by response surface methodology (RSM) for rapid analysis of bioactive compounds in the flower head of Chrysanthemum morifolium Ramat. *Ind. Crop Prod.* **2015**, *74*, 192–199.

41. Aboelazayem, O.; Gadalla, M.; Saha, B. Biodiesel production from waste cooking oil via supercritical methanol: Optimisation and reactor simulation. *Renew. Energ.* **2018**, *124*, 144–154.

42. Khajeh, M. Optimization of microwave-assisted extraction procedure for zinc and copper determination in food samples by Box-Behnken design. *J. Food Compos. Anal.* **2009**, *22*, 343–346.

43. Jaliliannosrati, H.; Amin, N.A.S.; Talebian-Kiakalaieh, A. Microwave assisted biodiesel production from *Jatropha curcas* L. seed by two-step in situ process: Optimization using response surface methodology. *Bioresour. Technol.* **2013**, *136*, 565–573.

44. Onyenkeadi, V.; Aboelazayem, O.; Saha, B. Systematic multivariate optimisation of butylene carbonate synthesis via CO_2 utilisation using graphene-inorganic nanocomposite catalysts. *Catal. Today* **2020**, *346*, 10–22.

45. Aboelazayem, O.; El-Gendy, N.S.; Abdel-Rehim, A.A.; Ashour, F.; Sadek, M.A. Biodiesel production from castor oil in Egypt: Process optimisation, kinetic study, diesel engine performance and exhaust emissions analysis. *Energy* **2018**, *157*, 843–852.

46. El-Gendy, N.S.; El-Gharabawy, A.A.S.A.; Amr, S.S.A.; Ashour, F.H. Response surface optimization of an alkaline transesterification of waste cooking oil. *Int. J. ChemTech Res.* **2015**, *8*, 385– 398.

47. El-Gendy, N.S.; Deriase, S.F.; Hamdy, A. The Optimization of Biodiesel Production from Waste Frying Corn Oil Using Snails Shells as a Catalyst. *Energ. Source Part A* **2014**, *36*, 623–637.

48. Long, X.; Cai, L.; Li, W. RSM-based assessment of pavement concrete mechanical properties under joint action of corrosion, fatigue, and fiber content. *Constr. Build. Mater.* **2019**, *197*, 406–420.

49. Mohammadifard, H.; Amiri, M.C. On tailored synthesis of nano CaCO3 particles in a colloidal gas aphron system and evaluating their performance with response surface methodology for heavy metals removal from aqueous solutions. *J. Water Environ. Nanotechnol* **2018**, *3*, 141–149.

50. Ambroziak, K.; Mbeleck, R.; Saha, B.; Sherrington, D.C. Greener and Sustainable Method for Alkene Epoxidations by Polymer-Supported Mo(VI) Catalysts. *Int. J. Chem. React. Eng.* **2010**, *8*, 1–13.

51. Bhuiyan, M.M.R.; Mohammed, M.L.; Saha, B. Greener and Efficient Epoxidation of 1,5-Hexadiene with *tert*-Butyl Hydroperoxide (TBHP) as an Oxidising Reagent in the Presence of Polybenzimidazole Supported Mo(VI) Catalyst. *Reactions* **2022**, *3*, 537–552.

52. Mohammed, M.L.; Mbeleck, R.; Patel, D.; Niyogi, D.; Sherrington, D.C.; Saha, B. Greener and efficient epoxidation of 4-vinyl-1-cyclohexene with polystyrene 2-(aminomethyl)pyridine supported Mo(VI) catalyst in batch and continuous reactors. *Chem. Eng. Res. Des.* **2015**, *94*, 194–203.

53. Olaniyan, B.; Saha, B. Multiobjective Optimization for the Greener Synthesis of Chloromethyl Ethylene Carbonate by CO₂ and Epichlorohydrin via Response Surface Methodology. *Energies* **2020**, *13*, 741.

54. Bhuiyan, M.M.R.; Saha, B. Optimisation of greener and more efficient 1,7-octadiene epoxidation catalysed by a polymer-supported Mo(VI) complex via response surface methodology. *React. Chem. Eng.* **2024**, *9*, 1036–1046.